Current-induced nonequilibrium vibrations in single-molecule devices

Jens Koch,[1] Matthias Semmelhack,[1] Felix von Oppen,[1] and Abraham Nitzan[2]

[1]*Institut für Theoretische Physik, Freie Universität Berlin, Arnimallee 14, 14195 Berlin, Germany*
[2]*School of Chemistry, The Sackler Faculty of Science, Tel Aviv University, Tel Aviv 69978, Israel*

(Dated: April 5, 2005)

Finite-bias electron transport through single molecules generally induces nonequilibrium molecular vibrations (phonons). By a mapping to a Fokker-Planck equation, we obtain analytical scaling forms for the nonequilibrium phonon distribution in the limit of weak electron-phonon coupling λ within a generic model. Remarkably, the width of the phonon distribution diverges as $\sim \lambda^{-\alpha}$ when the coupling decreases, with voltage-dependent, non-integer exponents α. We discuss the implications of this result for the current-induced dissociation of molecules.

PACS numbers: 73.23.Hk, 73.63.-b, 81.07.Nb, 05.70.Ln

Introduction.—The vision of molecular electronics [1] in part depends on the realization of devices such as molecular transistors, switches, or diodes. One strategy towards this goal involves the coupling of electronic and vibrational (phononic) degrees of freedom of molecules. Experiments with single-molecule devices have demonstrated effects of electron-phonon coupling in current-voltage characteristics (IVs) [2, 3, 4], and a number of theoretical studies have investigated such features in IVs [5, 6, 7, 8, 9, 10], shot noise [6, 10], and the thermopower [11] as well as applications such as diodes [12] and switches [13].

A question of principal importance for single-molecule devices are the consequences of nonequilibrium effects at finite bias. Strong nonequilibrium molecular vibrations can be beneficial in molecular devices, e.g., by enhancing switching rates between molecular conformations. In other instances, they may hinder the operation of devices, in the extreme case by inducing dissociation of the molecule. Recent theoretical work shows that even within simple models, vibrational nonequilibrium has important effects on IVs and shot noise [6, 14], may induce a shuttling instability [15, 16], or lead to current flow characterized by a self-similar hierarchy of avalanches of large numbers of transferred electrons [10].

Recent numerical results by Mitra et al. [6] suggest that intriguingly, vibrational nonequilibrium becomes stronger as the electron-phonon coupling λ *decreases*. Characterizing the vibrational nonequilibrium by the probability distribution of phonon excitations, these authors observe that the width of this distribution grows with decreasing coupling λ. In this paper, we develop an analytical theory of the phonon distribution which relies on a mapping to a Fokker-Planck equation. This mapping, which becomes exact in the limit of weak electron-phonon coupling, predicts in the absence of direct vibrational relaxation that the width at half maximum (WHM) of the phonon distribution diverges as $\lambda \to 0$. Remarkably, the WHM is shown to scale as $\lambda^{-\alpha}$ with bias-dependent, non-integer exponents $\alpha > 0$. We confirm our analytical results by numerical simulations.

We also discuss various extensions of the model which may be important for an accurate description of experimental systems. We study how the power-law divergence of the width of the phonon distribution is affected by direct vibrational relaxation. To assess the consequences of anharmonic potential surfaces, we extend our numerical simulations to phonon dynamics described by a Morse potential. Specifically, we show in this context that the current-induced dissociation rate is governed by an interplay of the above-mentioned divergence of the width of the phonon distribution and the slowing down of the diffusion in phonon space as λ decreases.

Model.—We investigate the nonequilibrium vibrational properties of a molecule coupled to metallic source and drain electrodes under finite bias. Electronic transport is taken to result from sequential tunneling through one spin-degenerate molecular orbital with energy ε, which is measured relative to the zero-bias Fermi energies of the leads and which can be tuned by a gate voltage. For clarity, we consider a single vibrational mode with frequency ω. The system's Hamiltonian reads $H = H_{\rm mol} + H_{\rm leads} + H_{\rm mix}$ [6, 11, 17, 18], where

$$\begin{aligned} H_{\rm mol} =& \varepsilon n_d + \frac{U}{2} n_d(n_d-1) \\ &+ \lambda\hbar\omega(b^\dagger + b)n_d + \hbar\omega(b^\dagger b + 1/2) \end{aligned} \tag{1}$$

describes the molecular degrees of freedom, $H_{\rm leads}$ a free electron gas in the leads $a = L, R$ (with creation operators $c^\dagger_{a\mathbf{p}\sigma}$), and $H_{\rm mix} = \sum_{a=L,R}\sum_{\mathbf{p},\sigma}\left(t_a c^\dagger_{a\mathbf{p}\sigma} d_\sigma + \text{h.c.}\right)$ the tunneling between leads and molecule.

We focus on the regime of strong Coulomb blockade, appropriate when voltage and temperature are small compared to the charging energy U. The operator d_σ ($d^\dagger_\sigma$) annihilates (creates) an electron with spin projection σ on the molecule, $n_d = \sum_\sigma d^\dagger_\sigma d_\sigma$ denotes the corresponding occupation-number operator. Vibrational excitations are annihilated (created) by b ($b^\dagger$). The electron-phonon coupling term can be eliminated by a canonical transformation [6, 17], leading to a renormalization of the parameters ε and U, and of the lead-molecule coupling $t_a \to t_a \exp[-\lambda(b^\dagger - b)]$. From now on, we refer to the

renormalized parameters as ε and U.

The coupling between molecule and leads is parameterized by the tunneling matrix elements t_L and t_R, and it is assumed to be weak in the sense that the energy broadening γ of molecular levels is small, i.e. $\gamma \ll k_BT, \hbar\omega$, so that a perturbative treatment for $H_{\rm mix}$ in the framework of rate equations is appropriate. We focus on temperatures $k_BT \ll \hbar\omega$ (corresponding to typical low-temperature experiments, e.g. [3]). For simplicity, we assume a symmetric device with $t_L = t_R \equiv t_0$ and identical voltage drops of $V/2$ across each junction.

Then, the occupation probability P_q^n for the molecular state $|\, n, q\,\rangle$ with n electrons and q phonons is determined by the rate equations

$$\frac{dP_q^n}{dt} = \sum_{n',q'} \left[P_{q'}^{n'} W_{q'\to q}^{n'\to n} - P_q^n W_{q\to q'}^{n\to n'} \right]. \qquad (2)$$

(The discussion of direct phonon relaxation is deferred until later in this paper.) The transition rates $W_{q\to q'}^{n\to n'}$ obtained by Fermi's golden rule are proportional to the square of the Franck-Condon (FC) matrix element

$$M_{q\to q'} = \int_{-\infty}^{\infty} dx\, \phi_{q'}(x)\phi_q(x - \sqrt{2}\lambda\ell_{\rm osc}), \qquad (3)$$

i.e. the overlap of two harmonic oscillator wavefunctions $\phi_q(x)$, shifted relative to each other by a distance $\sqrt{2}\lambda\ell_{\rm osc}$, with electron-phonon coupling strength λ, and vibrational oscillator length $\ell_{\rm osc} = (\hbar/M\omega)^{1/2}$. The FC matrix elements can be expressed in terms of generalized Laguerre polynomials, e.g. [11].

Phonon distributions for weak electron-phonon coupling.—For $\lambda \ll 1$, Eq. (3) leads to

$$|M_{q_1\to q_2}|^2 \simeq \frac{Q!}{q!}\frac{\lambda^{2\Delta q}}{(\Delta q!)^2}, \qquad (4)$$

valid for $q\lambda^2$, $\Delta q\lambda^2 \ll 1$, where $Q = \max\{q_1, q_2\}$, $q = \min\{q_1, q_2\}$, and $\Delta q = Q - q$. Therefore, the FC matrix elements and the transition rates $W_{q\to q'}^{n\to n\pm 1}$ decay rapidly with increasing Δq. Consequently, the vibrational state of the molecule is predominantly changed by processes for which $q \to q' = q \pm 1$, and $\Delta q = 1$. Neglecting all other processes, Eq. (2) describes a random walk in the space of phonon states q with q-dependent nearest-neighbor hopping rates. In this approximation, the random walker would eventually escape to infinity, as the rates for $q \rightleftharpoons q+1$ are equal and grow with q. This implies that there is *no steady-state* phonon distribution $P_q = \sum_n P_q^n$ within this random-walk model.

To derive the actual steady-state phonon distribution, it is therefore imperative to go beyond the random-walk model by including higher-order processes with $\Delta q > 1$. These may favor vibrational de-excitation processes since the applied voltage sets an upper limit to the increase (but not to the decrease!) in the vibrational excitation q by a tunneling event. For example, for $\epsilon = 0$ the full voltage drop $eV/2$ per sequential-tunneling event can be converted into vibrational energy. Thus, $\Delta q_a = \lfloor eV/2\hbar\omega \rfloor + 1$ is the leading-order asymmetric process *for which only de-excitation processes are permitted*. (Here, $\lfloor r \rfloor$ denotes the largest integer smaller or equal to r.)

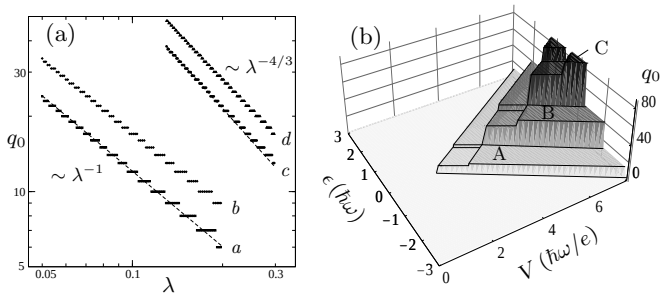

FIG. 1: (a) Scaling behavior of the phonon distribution width as a function of electron-phonon coupling for representative values of $(eV/\hbar\omega, \epsilon/\hbar\omega)$ equal to a: $(3,0)$; b: $(5,1)$; c: $(5,0)$; d: $(7,1)$. (b) Width of the phonon distribution as a function of bias and gate voltage at $\lambda = 0.15$ and $k_BT = 0.005\hbar\omega$. The scaling of the width differs for the plateaus according to A: $q_0 \sim \lambda^{-1}$, B: $q_0 \sim \lambda^{-4/3}$, and C: $q_0 \sim \lambda^{-3/2}$.

We can now derive the scaling of the steady-state phonon distribution P_q with electron-phonon coupling λ by balancing the diffusion process due to tunneling events with $\Delta q = 1$ [with diffusion constant $\sim q\lambda^2$, see Eq. (4)] and the leading asymmetric drift process [with rate $(q\lambda^2)^{\Delta q_a}$, see Eq. (4)]. This leads to the balance equation $q\lambda^2 P_q{}'' \sim (q\lambda^2)^{\Delta q_a} P_q{}'$ which implies a scaling law for the width q_0 of P_q, namely

$$q_0 \sim \lambda^{-\alpha}, \qquad \alpha = 2(\Delta q_a - 1)/\Delta q_a. \qquad (5)$$

This power-law scaling is nicely confirmed by numerical results for P_q as shown in Fig. 1(a). Remarkably, for $k_BT \ll \hbar\omega$ the discrete dependence of the leading asymmetric process on bias and gate voltage implies finite regions in the (V, ϵ)-plane characterized by certain *non-integer* exponents α. This "phase diagram" is shown in Fig. 1(b) where the wedge-shaped regions A, B, and C correspond to $\alpha = 1, 4/3$, and $3/2$, respectively [24].

For the diamond-shaped regions along the line $\epsilon = 0$ in Fig. 1(b), we can go beyond the derivation of this scaling behavior and obtain analytical results for the entire phonon distribution P_q by a mapping to a Fokker-Planck equation. The derivation exploits the crucial observation that for $U \to \infty$ and $k_BT \ll \hbar\omega$, the transition rates $W_{q\to q'}^{n\to n'} = s^{n\to n'} w_{q\to q'}$ factorize into a spin factor $s^{n\to n'} = (1 + \delta_{n',1})\delta_{|n-n'|,1}$ and a phonon factor $w_{q\to q'} = \tau_0^{-1} |M_{q\to q'}|^2 [\theta(q+\Delta q_a-1-q')+\theta(q-q'-\Delta q_a)]$, where $\tau_0^{-1} = \gamma/\hbar = 2\pi\rho\,|t_0|^2/\hbar$. In the stationary case, this implies the factorization $P_q^n = P^n P_q$, which allows us to derive the *purely phononic* rate equation

$$0 = dP_q/dt = \sum_{q'} [P_{q'} w_{q'\to q} - P_q w_{q\to q'}], \qquad (6)$$

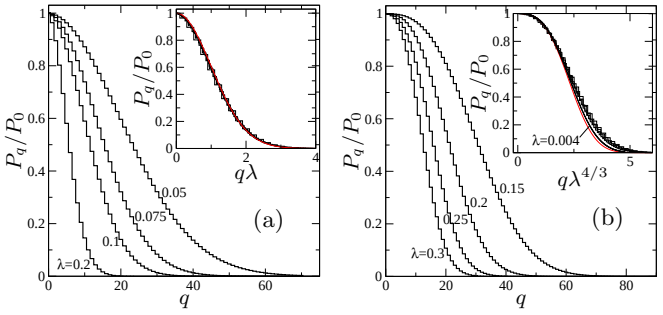

FIG. 2: (Color online) Phonon distributions P_q at bias voltages (a) $eV = 3\hbar\omega$ and (b) $eV = 5\hbar\omega$, plotted for several coupling strengths λ at $\epsilon = 0$, $k_BT = 0.05\hbar\omega$. The insets show that these distributions (approximately) collapse to universal curves given by the smooth curves (in red), which are the solutions of the the Fokker-Planck equation (7) specific to each voltage range $n\hbar\omega < eV/2 < (n+1)\hbar\omega$.

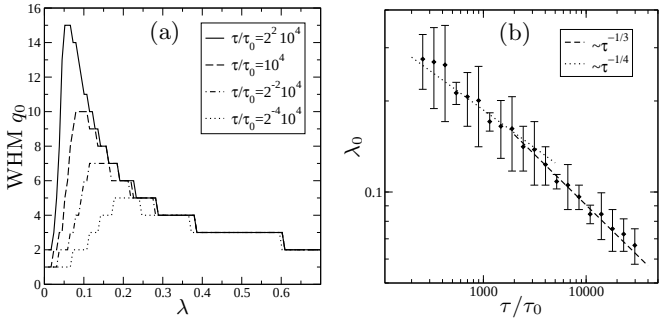

FIG. 3: (a) Width of the phonon distribution as a function of electron-phonon coupling strength for several vibrational relaxation times τ and $eV = 3\hbar\omega$, $k_BT = 0.05\hbar\omega$, $\epsilon = 0$. For $\lambda > 0.25$ all curves show the approximate $q_0 \sim \lambda^{-1}$ scaling. Below a relaxation-rate dependent crossover-point λ_0 the WHM is strongly suppressed due to direct relaxation. (b) Crossover-point λ_0 vs. relaxation time τ.

Since the phonon distribution becomes wide, we can take q to be continuous, expand $P_{q'}$ around $q' = q$ up to second order, and keep only the leading-order contributions to diffusion and drift. In this way we obtain the Fokker-Planck equation

$$0 = \frac{\partial P}{\partial t} = \frac{1}{2}\frac{\partial^2}{\partial q^2}\left[D(q)P(q)\right] - \frac{\partial}{\partial q}\left[A(q)P(q)\right], \qquad (7)$$

with diffusion coefficient $D(q) = 2q\lambda^2/\tau_0$, drift coefficient $A(q) = [\lambda^2 - c(q\lambda^2)^{\Delta q_a}]/\tau_0$, and $c = 2\Delta q_a(\Delta q_a!)^{-2}$. Remarkably, the stationary Fokker-Planck equation (7) can be solved analytically for any Δq_a by the scaling ansatz $P_q = a\lambda^\alpha f(\lambda^\alpha q)$ with a normalization constant a. The universal function f is uniquely determined by Eq. (7) together with the boundary conditions $f(0) = 1$, $f'(0) = 0$, and we find

$$f(x) = \exp\left[-x^{\Delta q_a}/b\right] \qquad (8)$$

with $b = \frac{1}{2}(\Delta q_a!)^2$. Note that in particular, this analytical result confirms the power-law scaling (5) of the width of the phonon distribution.

The power-law scaling (5) together with the analytical phonon distributions (8) constitute the central results of this paper. The phonon distributions are nicely confirmed by numerical solutions of the full rate equations as shown in Fig. 2 [25]. Therefore, we find that in fully developed nonequilibrium, the width of the phonon distribution *diverges* with *decreasing* electron-phonon coupling λ. The resulting phonon distributions are *non-analytic* in λ which implies that any naive perturbation theory in this parameter is inadequate.

Effects of direct vibrational relaxation.—Direct phonon relaxation can be included within the relaxation-time approximation by adding $-\frac{1}{\tau}[P_q^n - P_q^{\rm eq}\sum_{q'} P_{q'}^n]$ to the r.h.s. of the rate equations (2). Here, $P_q^{\rm eq}$ denotes the equilibrium phonon distribution, which can be approximated by $P_q^{\rm eq} = \delta_{q,0}$ for $k_BT \ll \hbar\omega$.

To understand the effect of direct vibrational relaxation on the phonon distribution P_q, it is important to note that the diffusion and drift processes in phonon space slow down as the electron-phonon coupling λ decreases. As λ decreases, we therefore expect that there exists a crossover coupling λ_0: For $\lambda \gg \lambda_0$, the vibrational diffusion is limited by the drift in phonon space induced by the asymmetry between vibrational excitation and de-excitation, as discussed above. By contrast, for $\lambda \ll \lambda_0$, the dominant limiting process is direct vibrational relaxation, leading to a decrease of the width of the phonon distribution. This expectation is confirmed by numerical results as seen in Fig. 3(a) which shows the width of the phonon distribution as a function of λ for various relaxation rates. Fig. 3(b) shows the dependence of λ_0 on relaxation time τ for $\Delta q_a = 1$. Note that λ_0 grows only very slowly with increasing relaxation. While the λ_0 vs. τ dependence is close to a power law with an exponent 1/4 - 1/3, no simple scaling can be expected. The reason is that the scaling suggested by the rate equation (2) amended by the relaxation term is incompatible with the scaling implied by the boundary condition $\lambda^{2(\alpha+1)} f'(0) = -\tau_0/\tau Sa$ at $q = 0$, where $S = 1 + P^0$.

Morse potential and dissociation.—So far, our considerations were based on the harmonic approximation for the phonon potential. We argue however that wide phonon distributions are not an artefact of this approximation, but also appear for more realistic, anharmonic potentials. As an example, we investigate the effect of weak electron-phonon coupling for the Morse potential $V(x) = D\left[e^{-2\beta(x-x_0)} - 2e^{-\beta(x-x_0)}\right]$, where $D > 0$ denotes the dissociation energy, β the inverse range, and x_0 the potential minimum. The Morse potential [19] accurately describes the vibrations of diatomic molecules and allows us to study current-induced molecular dissociation [20, 21]. In analogy to the harmonic oscillator

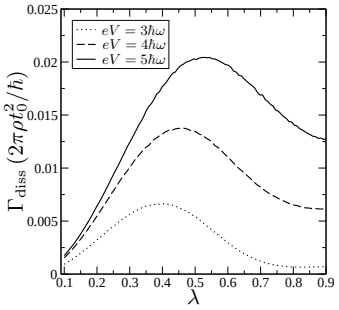

FIG. 4: Mean dissociation rate as a function of electron-phonon coupling strength at $k_BT = 0.005\hbar\omega$ for several bias voltages as obtained by Monte Carlo simulation with a Morse potential containing 10 bound states.

model, we assume that the potential energy curves for the neutral and singly-charged molecule have the same shape (i.e. D and β are fixed), but are shifted with respect to each other by $\Delta x = \sqrt{2}\lambda\ell_{\rm osc}$. Building on e.g. Ref. [22], we derive Franck-Condon matrix elements for the Morse potential, analogous to Eq. (3), between bound states as well as between bound and continuum states.

Specifically, we study the current-induced dissociation rate of the molecule as function of electron-phonon coupling and bias voltage by Monte-Carlo simulation. Assuming low temperatures and switching on the voltage at $t = 0$, the molecule starts in the phonon ground state and then evolves in time due to the tunneling dynamics. Given that transitions from the continuum back to bound states are negligible, we obtain an average dissociation rate $\Gamma_{\rm diss}$ by recording the times $t_{{\rm diss},i}$ required for reaching the continuum and averaging over samples. (We note that calculations of mean first-passage times for the highest-lying bound level give compatible dissociation times.) Typical results for dissociation rates for weak electron-phonon couplings (without relaxation) are depicted in Fig. 4.

The maximum in the dissociation rate $\Gamma_{\rm diss}$ vs. λ can be understood as a direct consequence of a competition between the broadening of the phonon distribution and the slowing down of diffusion in phonon space. As λ decreases from values of the order of unity, $\Gamma_{\rm diss}$ first increases. This reflects the concurrent increase in the width of the phonon distribution. Beyond the maximum, $\Gamma_{\rm diss}$ decreases due to the slowing down of diffusion in phonon space. Finally, the dissociation rate increases with voltage because of the increased width of the phonon distribution (see Fig. 1) and the possibility of multiple-phonon excitations within one tunneling event.

Conclusions.—We have studied the current-induced vibrational nonequilibrium in single-molecule devices and found that remarkably, the width of the nonequilibrium phonon distribution increases with decreasing electron-phonon coupling. We have identified regions in the bias voltage-gate voltage plane in which the width of the phonon distribution exhibits power-law divergences with decreasing λ, with voltage-dependent non-integer exponents. In some representative cases, we are able to derive analytical phonon distributions by a mapping to a Fokker-Planck equation. These dramatic effects of current-induced nonequilibrium are found to have important implications in more realistic models which include direct vibrational relaxation and anharmonic potential surfaces. A very important conclusion from our work is that approaches which are perturbative in the electron-phonon coupling λ have to be assessed with extreme care in fully-developed nonequilibrium. Finally, we remark that recent experiments [23] show that the vibrational relaxation time can be as large as 10ns, in which case current-induced vibrational nonequilibrium becomes important for currents as small as 10pA.

This work was supported in part by Sfb 658, the Junge Akademie (FvO), Studienstiftung des deutschen Volkes (JK), and the Israel Science Foundation (AN).

[1] A. Aviram and M. Ratner, Chem. Phys. Lett. **29**, 277 (1974).
[2] H. Park, J. Park, A. K. L. Lim, E. H. Anderson, A. P. Alivisatos, and P. L. McEuen, Nature **407**, 57 (2000).
[3] R. H. M. Smit, Y. Noat, C. Untiedt, N. D. Lang, M. C. van Hemert, and J. M. van Ruitenbeek, Nature **419**, 906 (2002).
[4] L. Yu, Z. Keane, J. Ciszek, L. Cheng, M. Stewart, J. Tour, and D. Natelson, Phys. Rev. Lett. **93**, 266802 (2004).
[5] K. D. McCarthy, N. Prokof'ev, and M. T. Tuominen, Phys. Rev. B **67**, 245415 (2003).
[6] A. Mitra, I. Aleiner, and A. J. Millis, Phys. Rev. B **69**, 245302 (2004).
[7] S. Braig and K. Flensberg, Phys. Rev. B **70**, 085317 (2004).
[8] M. Galperin, M. A. Ratner, and A. Nitzan, Nano Lett. **4**, 1605 (2004).
[9] Y.-C. Chen, M. Zwolak, and M. DiVentra, Nano Lett. **4**, 1709 (2004).
[10] J. Koch and F. von Oppen, cond-mat/0409667 (2004).
[11] J. Koch, F. von Oppen, Y. Oreg, and E. Sela, Phys. Rev. B **70**, 195107 (2004).
[12] G. A. Kaat and K. Flensberg, cond-mat/0411173 (2004).
[13] M. Cizek, M. Thoss, and W. Domcke, cond-mat/0411064 (2004).
[14] V. Aji, J. E. Moore, and C. M. Varma, cond-mat/0302222 (2003).
[15] D. Fedorets, L. Gorelik, R. I. Shekhter, and M. Jonson, Phys. Rev. Lett. **92**, 166801 (2004).
[16] T. Novotný, A. Donarini, C. Flindt, and A.-P. Jauho, Phys. Rev. Lett. **92**, 248302 (2004).
[17] L. I. Glazman and R. I. Shekhter, Sov. Phys. JETP **67**, 163 (1988).
[18] D. Boese and H. Schoeller, Europhys. Lett. **54**, 668 (2001).
[19] P. M. Morse, Phys. Rev. **34**, 57 (1929).
[20] B. C. Stipe, M. A. Rezaei, W. Ho, S. Gao, M. Persson,

and B. I. Lundqvist, Phys. Rev. Lett. **78**, 4410 (1997).
[21] For a recent review, see T. Seideman, J. Phys.: Condens. Matter **15**, R521 (2003).
[22] R. Lemus, J. M. Arias, and J. Gómez-Camacho, J. Phys. A **37**, 1805 (2004).
[23] B. LeRoy, S. Lemay, J. Kong, and C. Dekker, Nature **432**, 371 (2004).
[24] Additional smaller steps can be traced back to changes in the nature of the asymmetry within one scaling phase.
[25] The small deviations observed in the inset of Fig. 2(b) reflect that the effective perturbation parameter $q_0\lambda^2 \sim \lambda^{2/(\Delta q_a)}$ grows with Δq_a even at fixed λ.